

## PRELIMINARY RESULTS ON THE GLACIAL WINDS REGIME OF THE MANDRONE GLACIER

M. Falocchi<sup>1</sup>, S. Barontini<sup>1</sup>, G. Grossi<sup>1</sup> & R. Ranzi<sup>1</sup>

(1) Dipartimento di Ingegneria Civile Architettura Territorio e Ambiente, Università di Brescia, Italia, e-mail: marco.falocchi@ing.unibs.it, barontin@ing.unibs.it, giovanna.grossi@ing.unibs.it, ranzi@ing.unibs.it

### ABSTRACT

*During the summer of 2008, from 13 June to 29 September, at an altitude of 2780 m asl, a micro-meteorological station was placed on the Mandrone Glacier (Adamello Group, Italian Central Alps) by a team of the University of Brescia. The aim of the MandronEX (Mandrone EXperiment) field campaign was the collection of useful data to analyse the glacial winds and estimate the mass balance of the glacier. In this study will the data recorded by the 3 axes Gill WindMaster sonic anemometer at a sampling rate of 20 Hz, during the first nine days of the experiment will be analysed, in order to detect the glacial winds. A general description of the atmospheric pressure, the air temperature and the wind directions was provided in order to understand the meteorological conditions on the glacier and to obtain preliminary information about the winds regime. The more accurate elaborations executed by means of the frequency analysis and the wind-roses have shown an alternate regime of anabatic winds, from the valley to the glacier, especially in the first days of the campaign, and katabatic ones from the glacier to the valley. The spectral analysis of the  $u$  and  $w$  wind speed components, instead, allowed to detect the presence of the  $-5/3$  slope Kolmogorov law, in the inertial sub-range. Moreover, according to the analysis provided by Kaimal et al. (1972) the atmosphere seems to be stable during the investigated period.*

### 1 INTRODUCTION

On the Mandrone Glacier, during the summer of 2008 a glacio-meteorological field campaign was carried out by the University of Brescia. This experiment, called MandronEX (Mandrone EXperiment), aimed at studying the impact of the climate on the water resources within the Adamello Natural Park. Because during the melting period the surface of the glacier is close to the melting temperature, the glaciers become sensitive indicators of climatic changes. Measurements and models based on their mass and energy balance are therefore the best way to infer such changes (Oerlemans, 1994). A micrometeorological station was placed for this reason at the height of 2780 m a.s.l. to collect useful data to estimate the energy balance for the 2008 summer and thus completing a series of twelve years (1995–2006) by applying the PDSLIM energy-balance model (Ranzi et al., 2010). Other relevant results that can be obtained by the data collected concerns the analysis of the dynamics of the air masses. In fact on a glacier it has been observed that usually takes place a particular kind of slope wind, generated by the negative buoyancy

between the snow or ice and the temperature of the air over it, known as glacial winds (Oerlemans & Grisogono, 2002).

In this study the preliminary results, obtained analysing the wind data collected in the first period of the MandronEX, *i.e.* from 14 to 21 June 2008 are presented and discussed. In these days it was observed the presence of both anabatic flowing from the valley to the mountains and vice-versa katabatic winds. Moreover, starting from the alternated situation between anabatic and katabatic winds the wind regime becomes almost purely katabatic with the increasing of the air temperature.

In order to complete the study, the spectra of the horizontal wind speed component Northward,  $u$  and the vertical wind speed component  $w$  has been computed to analyse their path in order to observe the inertial sub-range and compare them with the  $-5/3$  slope Kolmogorov law for homogeneous and isotropic turbulence. Following the work of Kaimal et al. (1972) the spectra have been normalised and then compared with the universal curves for the neutral atmospheric stability. In this way, during the investigated period, it was possible to observe the effect, of the meteorological occurrences at the synoptic-scale, on the wind regime and on the stability of the atmosphere.

## **2 THE SITE AND THE MANDRONEX CAMPAIGN**

The Adamello Glacier, located in the Central Italian Alps between the Provinces of Brescia and Trento, is the largest glacierised area in the Italian Alps with a total area of 17.4 km<sup>2</sup> (data retrieved from ASTER satellite image in 2003). The particular orographical configuration over which the glacier lies, allows to detect a central accumulation zone, known as "Pian di Neve" plateau, surrounded by the mean peak of Adamello (3539 m asl) and the secondary peaks of Corno Bianco at North, Dosson di Genova at East, Cima Adamé, Corni di Salarno and Corno Miller at South and Cima Ugolini at West. Between this peaks five glacial tongues take origins. For this peculiarity, following the traditional classification used in the Registry of the Italian Glacier (1952) the Adamello Glacier can be classified as a Scandinavian glacier. These glacial tongues also determine five hydrographic sub-basins: Miller Superiore, Salarno, Corni di Salarno, Adamé and Mandrone. The melting water of the first four ones supply the basin of the Oglio river and the complex hydroelectric power system of San Fiorano at Cedegolo (Province of Brescia). The Mandrone glacier, instead behaves as a valley glacier and it supplies the Sarca river. It is the largest glacial tongue of the Adamello Glacier with a surface of 13.38 km<sup>2</sup> (ASTER 2003) and it flows between the Corno Bianco and the Dosson di Genova from SW to NE in the Val di Genova.

Along the Mandrone, on 13 June 2008 a micrometeorological station was placed, at the altitude of 2780 m asl, by a team of the University of Brescia with the aim of collecting useful data to analyse glacial winds and estimate the energy and mass balance of the glacier (Figure 1). This station was equipped with two different type of devices: traditional ones, characterised by a low frequency acquisition rate of 1 Hz and innovative ones, with an high acquisition frequency of 20 Hz. The latter were an ultrasonic anemometer and a gas analyser. The ultrasonic anemometer was a 3 Axes Gill WindMaster, placed at the height of about 3 m above the surface, while the gas analyser was a Licor Li-7500.

Measurements began in the evening of 13 June and lasted until noon of 29 September, however high quality and complete data sets were available only for some periods. In fact,

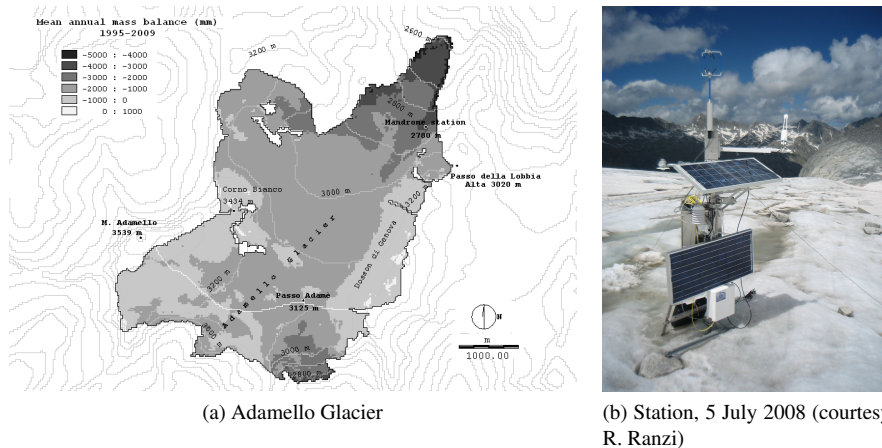


Figure 1: The Adamello Glacier mass balance obtained with the PDSLIM model Ranzi et al. (2010) and the micro-meteorological station on the Mandrone Glacier, on the right.

the presence of malfunctioning sources makes it difficult to obtain long and continuous series of complete data sets. This behaviour is even emphasised when the measurements are carried out over glaciers, because under the effect of the glacial movements and the melting of the surface it is difficult to guarantee a vertical fixed position to the station. Moreover the sensors can be covered by a frost layer, that is the reason of their frequent break-down, gaps or meaningless data (Weber, 2007).

In this study the attention will be focused on the first eight days of experimental field campaign: from 14 to 22 June, when the anemometer was placed in vertical position. Because the wind regime is strongly influenced by the meteorological conditions, in particular by the occurrence of atmospheric disturbances and the temperature regime (Arya, 1988), before proceeding to the quantitative analysis it is necessary to provide a qualitative overview of the meteorological conditions during the investigated period.

In Figure 2 the planar wind speed and wind direction are represented together with the atmospheric pressure and the air temperature, in order to qualitatively assess the meteorology conditions. Before looking at the pressure series, it should be accounted that being at high altitude, contained fluctuations can correspond to relevant meteorological changes. In this case the low values of the pressure at the begin of the campaign are a sign of the presence of unstable weather conditions, confirmed by 15 cm snowfall measured by Ranzi in the night between 13 and 14 June, and the passage of a little atmospheric disturbance between the evening of the 15 and the morning of the 16 June. In the next days the pressure increases its value, characterising a high pressure period on the glacier.

The changing weather conditions due to synoptic-scale forcing have influenced both the temperature and the wind speed regimes. About the temperature, the lower observed value is registered at  $-5^{\circ}\text{C}$  and then almost constant temperature is observed around  $2\text{--}3^{\circ}\text{C}$  until 18 June. Only in the following days it is possible to observe the characteristic cycle between night and day, that fastly increases its maximum, reaching  $13^{\circ}\text{C}$  on 20 June. The plot of the wind shows a speed regime that is strongly disturbed at the beginning of the period of interest, when the low values of the atmospheric pressure occurred, while it

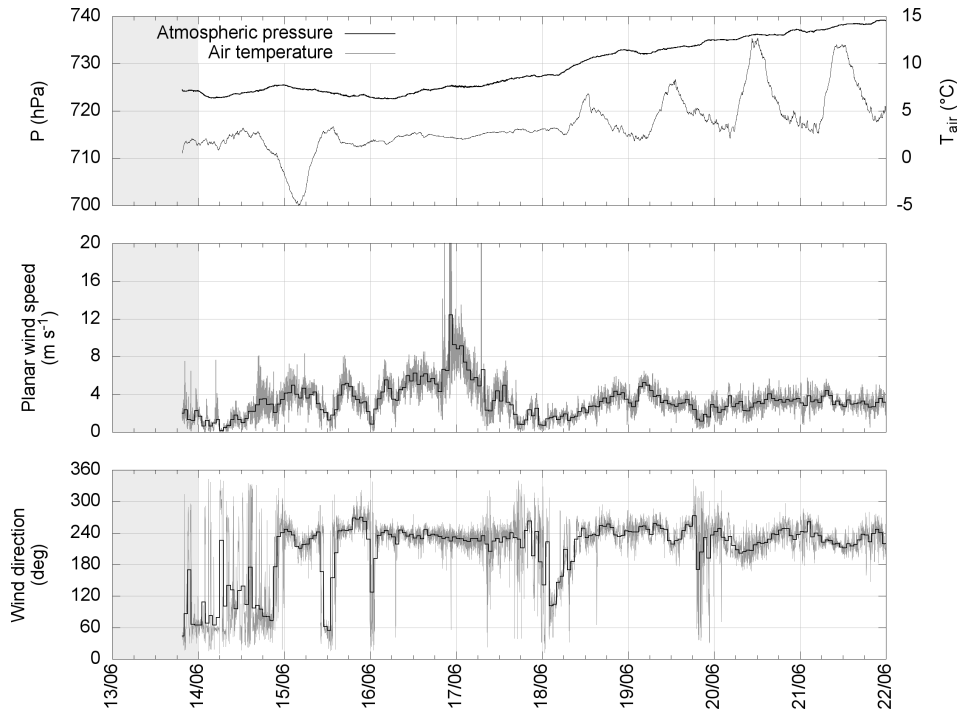


Figure 2: Atmospheric pressure, air temperature, planar wind speed and wind direction from the beginning of the campaign on 13 June at 19:25 to 22 June. The data used for the analysis are in the white area, while the data in the solid one were not used. The plots of the planar wind speed and wind direction show in grey lines the mean value of the meteorological variable at one minute, while the black ones are the one hour averaged values.

becomes more stable from 19 June, with the pressure increasing values.

Finally, the wind direction plot shows an alternation between anabatic and katabatic winds especially in the first three days. During the rest of the period the katabatic condition is dominant with respect to the anabatic one, that sometimes is still detectable. Such condition allows to suppose that the wind direction regime is more sensitive to the temperature one than the effects of the synoptic-scale forcing.

### 3 THE GLACIAL WINDS: DETECTION AND ANALYSIS

The data used in this first part of the study are the mean value over windows of 60 s (1200 data for each 60 s window), of the data collected by the anemometer. This choice was considered a good compromise in order to work with a lighter database, but without losing information on the minor fluctuations of speed and direction of the glacial winds. In order to detect, with more detail the presence of one or more preferential directions in the winds, which were already noted in the data series, a both persistence analysis and a planar wind-rose were represented, for all the days of the period from 14 to 21 June.

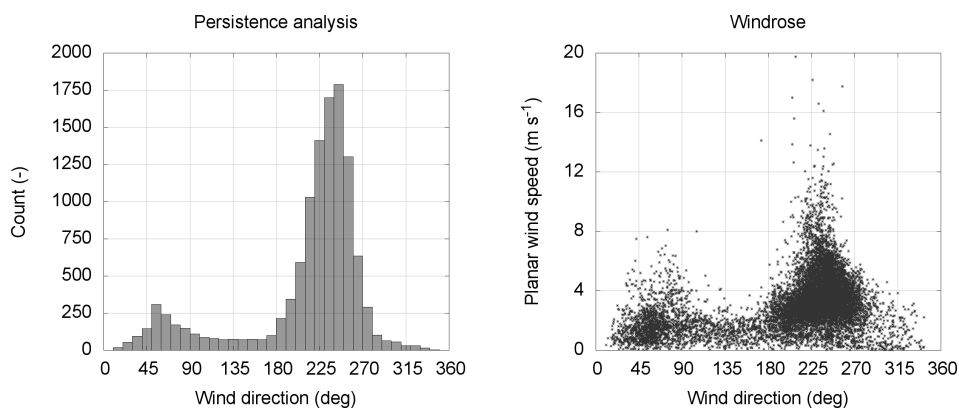


Figure 3: Persistence analysis (on the left) and Planar wind-rose (on the right) obtained analysing the data averaged at 60 s from the records of the anemometer.

The persistence can be defined in several way, in this case it was plotted as histograms according to Oerlemans (1998), with the number of the wind direction that falls in 36 equispaced classes of 10 degrees amplitude. The planar wind-rose, instead, is a scatter plot of wind direction against the wind speed.

The obtained results are shown in Figure 3. Here the wind directions are measured clockwise from the Northward axis. First of all, it is possible to observe the presence of two well defined peaks in both the plots around the direction between 50–60 degrees and 240–250 degrees, that is in agreement with the direction of the axes of the valley, where the station was placed. The difference between them is about 180 degrees, so it means that during the investigated period, both anabatic winds flowing from the valley up to the glacier and katabatic ones, from the glacier flow downslope occurred. However, because the numbers of the samples of the first peak (50–60 degrees, anabatic peak ) is lower than the second one, of about five times, it is possible to conclude that only during some days there was the alternation of the wind regime, after that the katabatic condition become dominant.

The wind-rose plot confirms the previous observations about the presence of a change in the wind directions. It also gives information about the mean wind speed, that for the anabatic winds is around  $2 \text{ m s}^{-1}$ , while for the katabatic ones it is characterised by a greater variability, ranging between  $2 \text{ m s}^{-1}$  and  $8 \text{ m s}^{-1}$ .

The daily wind-roses, plotted in Figure 4, allow to observe that at the beginning of the period of interest there is a clear alternation of the wind direction. This alternation decreases in the following days since the wind regime becomes purely katabatic during the last two days. This behaviour can be probably justified considering the different heating of the air masses on the glacier and in the Val di Genova. It is likely that at the beginning of the campaign, in the beneath valley, the buoyancy forces of the air was greater than the effect of cold air masses on the glacier, so that it was possible the formation of the anabatic winds. Paying the attention on the last days, moreover, it can be observed the presence of katabatic winds blowing in a range of direction between 200–270 degrees. This means that such winds are not drained along the principal axis of the valley but also from Pian di Neve which is at South–West with respect to the installed station.

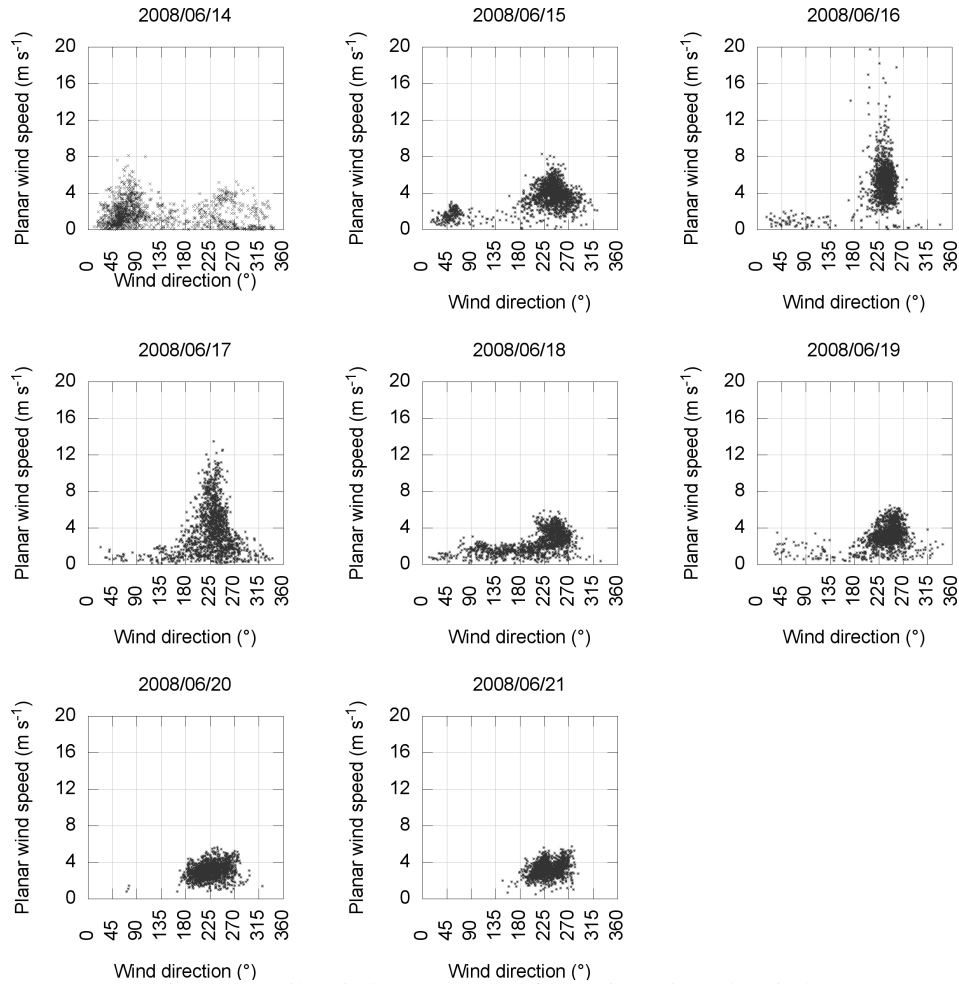


Figure 4: Daily wind-roses plotted for the investigated period.

#### 4 SPECTRAL ANALYSIS OF THE GLACIAL WINDS

The spectra  $S(f)$  (with  $f$  the cyclic frequency) of a sample of eighteen hours have been analysed for the planar Northward wind speed component  $u$  and vertical wind speed component  $w$ , in order to acquire more information about the behaviour of the glacial winds during the investigated period. The analysis was performed subdividing each hour, into five blocks of twelve minutes, to guarantee that the number of data is a power of two, as suggested in other studies (*e.g.* Smeets et al. (1998, 2000); Kaimal & Finnigan (1994)). In this way the extremes of the cyclic frequency domain are  $1.4 \cdot 10^{-3}$  Hz and 10 Hz (this is the Nyquist frequency for a 20 Hz sampled signal). Then the FFT (Fast Fourier Transform) and the needed corrections to remove the noise at the medium and high frequencies for each block, was implemented using the EddyPro software (Li-COR, 2011). At this stage, the representative spectrum for each hour was obtained averaging

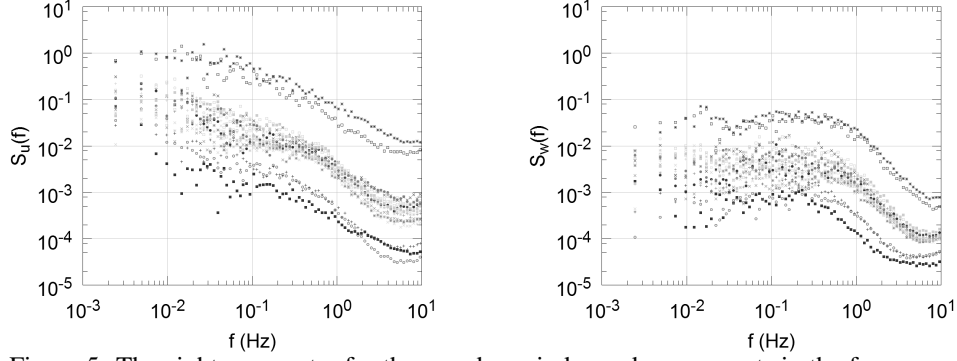


Figure 5: The eighteen spectra for the  $u$  and  $w$  wind speed components in the frequency space. Each spectrum must be intended as a mean spectrum, obtained averaging the spectra computed on the five blocks of 12 minutes, in which the respective hour has been divided.

the spectra of the respective five blocks.

The spectra of the  $u$  and  $w$  wind speed components plotted against the cyclic frequency  $f$  are shown in Figura 5. Here it can be observed that there are three well distinguished bands of spectra. The central one collects the greatest part of the computed spectra, when only katabatic winds are present, while in the upper and in the lower bands the spectra correspond to the period in which there were the alternation between the anabatic and katabatic wind regime.

Kaimal et al. (1972) showed that the normalised spectra of the turbulence in the surface layer can be reduced to a family of curves. Such normalised spectra are defined as:

$$\hat{S}(f) = \frac{S(f)}{u_*^2 \varphi_\epsilon^{-2/3}} \quad (1)$$

where  $u_*^2 = \langle u'w' \rangle$  is the squared friction velocity and  $\varphi_\epsilon^{-2/3}$  is the dimensionless dissipation rate, which is expressed by:

$$\varphi_\epsilon = \frac{kz\epsilon}{u_*^3} \quad (2)$$

with  $k$  is the von Kàrmàn constant equal to 0.4,  $z$  the height of the device from the ground and  $\epsilon = -\langle u'w' \rangle \frac{\partial \bar{u}}{\partial z}$  the rate of dissipation of the turbulent kinetic energy. The curves obtained by means of equation 1, and plotted against the dimensionless frequency,  $n$  provided by equation 3:

$$n = \frac{fz}{U} \quad (3)$$

with  $U$  the averaged wind speed in the interested interval, have the peculiarity to spread out at the low frequencies with the stability parameter:

$$\frac{z}{L} = kz \frac{g}{\theta} \left( \frac{T_*}{u_*^2} \right) \quad (4)$$

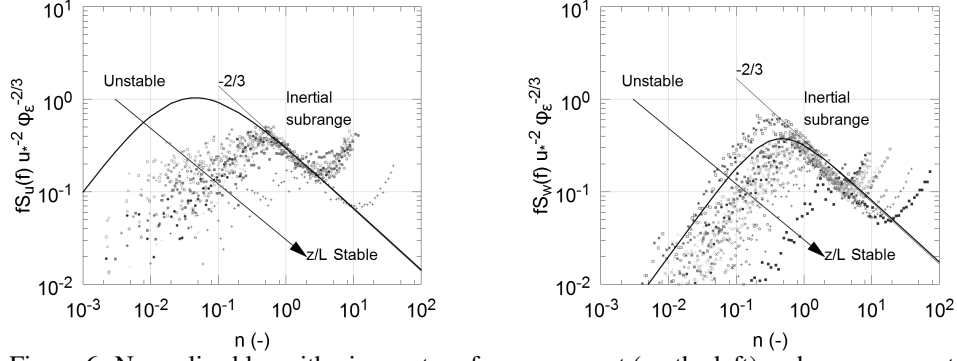


Figure 6: Normalised logarithmic spectra of  $u$  component (on the left) and  $w$  component (on the right) plotted against the dimensionless frequency  $n$ .

where  $L$  is the Obukov length,  $\bar{\theta}$  is the averaged potential temperature and  $T_* = -\langle w'\theta'u_*^{-1} \rangle$  is the scaling temperature. Moreover the spectra collapse into a single, universal function at the high frequencies, *i.e.* in the inertial subrange. In this range the curves are well approximated by the  $-5/3$  Kolmogorov power law, which expressed in the frequency domain assumes the form of a  $-2/3$  power law as reported in the following equation:

$$\frac{fS_\alpha(f)}{u_*^2} = \frac{\alpha_1}{(2\pi k)^{2/3}} \varphi_\epsilon^{2/3} n^{-2/3} \quad (5)$$

In equation 5  $\alpha_1$  is a parameter assuming values between 0.5 and 0.55. The  $\alpha_1$  parameter was assumed equal to 0.52, according to Smeets et al. (1998).

In agreement with the Monin–Obukov similarity theory, the dimensionless dissipation rate for turbulent energy can be written as an empirical function of the stability parameter, that can be found when the vertical gradients of temperature and  $w$  are known. However this information is not available for the MandronEX campaign, therefore a proportionality factor,  $\xi$ , between the normalised spectrum and the dimensionless frequency,  $n$  was defined, obtaining:

$$\xi = \frac{\alpha_1}{(2\pi k)^{2/3}} \varphi_\epsilon^{2/3} \quad (6)$$

The value of  $\xi$  was fitted against the dimensionless frequency in the inertial sub range by means of a power law with exponent  $-2/3$ , in order to estimate the unknown term and then to reconstruct the curves of Kaimal.

The Figure 6 shows the normalised spectra  $fS(f)u_*^{-2}\varphi_\epsilon^{-2/3}$  for the  $u$  and  $w$  wind speed components. Here it can be observed how the experimental spectra collapse into a unique curve that is well approximated by means of a power law in accordance to the Kolmogorov one.

The solid lines in the plots are the empirical curves for an atmosphere that is in neutral condition, which expressions are:

$$\frac{fS_u(f)}{u_*^2} = \frac{105n}{(1+33n)^{5/3}} \quad \text{and} \quad \frac{fS_w(f)}{u_*^2} = \frac{2n}{1+5.3n^{5/3}} \quad (7)$$



In the region below them are placed the spectra of a stable atmosphere, while the outer region is the space of the spectra recorded in an unstable atmosphere. This analysis allows to compare them to the experimental spectra found and then establish the atmospheric conditions. As it can be seen in the plot the spectra of the  $u$  component are always placed below the neutral condition curve, means that in period considered in this analysis the atmosphere was in stable conditions. On the other hand for the vertical wind speed  $w$  it can be observed that the spectra obtained are closer to the neutral condition than for the previous component. Then it seems that the  $w$  component of the wind speed is more sensitive to the instability than the  $u$  one.

## **5 CONCLUSIONS**

In this work the preliminary results on the glacier wind regime of the Mandrone Glacier (Adamello Group) observed during the MandronEX micrometeo–glaciological field campaign are presented, with the aim to monitoring energy fluxes and wind. To do this a micro–meteorological station was placed on the glacial tongue of the Mandrone Glacier at an altitude of 2780 m asl by a team of the University of Brescia. One of the installed devices was a ultrasonic anemometer (3 Axes Gill WindMaster) characterised by a sampling frequency of 20 Hz, which recorded, from the 14 to the 22 of June, the  $u$ ,  $v$  and  $w$  components of the wind speed.

After a brief presentation about the evolution of the meteorological conditions in the days of interest, that allowed to observe the end of a low pressure period followed by a high pressure one and the increase of the air temperature, the first observations about the regime of the wind were provided by means of the plot of the wind directions.

The first part of the study was performed by averaging the original data set every 60 s. The frequency analysis and the planar wind–rose confirms the presence of the alternation between anabatic and katabatic winds. Two well marked maxima, the highest for the directions of 200–270 degrees and the lowest between 50–60 degrees, with wind speed respectively ranging from 2 to 8 m s<sup>-1</sup> and 2 m s<sup>-1</sup>. The plots of the daily wind–roses show that at the beginning of the studied period there was an alternate regime of anabatic and katabatic winds that becomes purely katabatic in the last days. This effect was hypothesised to be related to the different heating of the air masses on the glacier and in the beneath valley and their buoyancy forces.

The spectral analysis of the  $u$  and  $w$  components of the wind speed was executed over eighteen hours, using the complete information collected by the sonic anemometer. It allowed to observe the pattern of the spectra and indicated the stability of the atmosphere by means of the normalised spectra, as suggested by Kaimal et al. (1972). Both  $u$  component and  $w$  component are stable, but the spectra of the  $w$  component approaches the neutral condition. It can be therefore observed how the effects of synoptic–scale forcing do not influence the anabatic–katabatic wind regime during the meteorological occurrences. As it was confirmed also in other studies, the glacial winds are governed by gravity, *e.g.* Van Den Broeke (1997), and in such conditions the turbulence is created in a stable or near–neutral surface layer.

## BIBLIOGRAPHY

- Arya, S. P. (1988). *Introduction to micrometeorology*, vol. 42 of *International Geophysics Series*. San Diego, California: Academic Press, Inc.
- Kaimal, J. C., & Finnigan, J. J. (1994). *Atmospheric Boundary Layer Flows. Their structure and measurement*. Oxford University Press.
- Kaimal, J. C., Wyngaard, J. C., Izumi, Y., & R., C. O. (1972). Spectral characteristics of the surface-layer turbulence. *Quarterly Journal of the Royal Meteorological Society*, 98, 563–589.
- Li-COR (2011). *EddyPro, Eddy Covariance Software, version 3.0*.
- Oerlemans, J. (1994). Quantifying global warming from the retreat of glaciers. *Science*, 264, 243–245.
- Oerlemans, J. (1998). *The atmospheric boundary layer over melting glaciers*. In: *Clear and Cloudy Boundary Layers*, chap. 6. Royal Netherlands Academy of Art and Sciences.
- Oerlemans, J., & Grisogono, B. (2002). Glacier winds and parametrisation of the related surface heat fluxes. *Tellus*, 54A, 440–452.
- Ranzi, R., Grossi, G., Gitti, A., & Taschner, S. (2010). Energy and mass balance of the Mandrone Glacier (Adamello, Central Alps). *Geografia Fisica e Dinamica Quaternaria*, 33(1), 45–60.
- Smeets, C. J. P. P., Duynkerke, P. G., & Vugts, H. F. (1998). Turbulence characteristics of the stable boundary layer over a mid-latitude glacier. Part I: a combination of katabatic and large-scale forcing. *Boundary Layer Meteorology*, 87, 117–145.
- Smeets, C. J. P. P., Duynkerke, P. G., & Vugts, H. F. (2000). Turbulence characteristics of the stable boundary layer over a mid-latitude glacier. Part II: pure katabatic forcing conditions. *Boundary Layer Meteorology*, 97, 73–107.
- Van Den Broeke, M. (1997). Structure and diurnal variation of the atmospheric boundary layer over a mid-latitude glacier in summer. *Boundary Layer Meteorology*, 87, 183–205.
- Weber, M. (2007). A parametrization for the turbulent fluxes over melting surfaces derived from eddy correlation measurements. *Proceeding Alpine Snow Workshop, National Park Berchtesgaden*, (17), 138–149.